Characterization of Deepwater Natural Gas Samples. Part 1: 78 % Methane Mixture with Heavy Components

M. Atilhan*

Department of Chemical Engineering, Qatar University, Doha, Qatar

S. Ejaz, J. Zhou, D. Cristancho, I. Mantilla, J. Holste, and K. R. Hall

Artie McFerrin Department of Chemical Engineering, Texas A&M University, College Station, TX

High-accuracy density measurement data are necessary to develop and validate equations of state (EoS) for use in custody transfer of natural gas through pipelines. The development of AGA8-DC92, which is the current industry standard EoS, used a databank of natural gas mixtures with compositions containing up to 0.2 mole fraction of the heavier C_{6+} fraction and should predict densities of natural gas mixtures containing higher mole fractions of the C_{6+} fraction with the same accuracy. With advances in exploration, drilling, and production, natural gas streams containing higher percentages of the C_{6+} fraction have become available from the deep-water and ultradeep-water Gulf of Mexico in recent years. High-accuracy density data for such natural gas mixtures are necessary to check if AGA8-DC92 covers the entire range of pressure, temperature, and composition encountered in custody transfer. An isochoric apparatus allows the performance of precise and fast measurements through a fully automated procedure over wide pressure and temperature ranges especially around the cricondentherm (CT) and the cricondenbar (CB) of the sample of interest. A systematic study in the vicinity of CT and CB for deep-water natural gas samples is extremely important. Accurate CT and CB measurements help the gas industry avoid retrograde condensation in natural gas pipelines. This work examines a synthetic natural gas sample containing 0.78 mole fraction of methane. A state-of-the-art, high-pressure, high-temperature, compact single-sinker magnetic suspension densimeter provides density measurements. A compact isochoric apparatus provides phase envelope measurements.

Introduction

Natural gas is the most environmentally friendly fossil fuel. Its proven reserves have increased yearly, and the development of new technologies allows exploration and recovery of nonconventional reservoirs whose compositions and characteristics differ from conventional ones.[1,2] Deep-water oil and gas reserves play a major role in North America's oil and gas supply containing 90 hydrocarbon production projects on line[3] in 2004. Improved technology has made ultradeep-water production a reality in North America. The largest capacity deep-water pipeline system ever built can transport more than 42 million cubic meters of gas when completed.[4] Deep-water gas can meet the rising demand for natural gas whose consumption may double worldwide by 2030.[5]

AGA8-DC92 is the current U.S. industry standard equation of state (EoS) for natural gas custody transfer. However, the compositions of natural gas mixtures from deep-water and ultradeep-water production are different from those used to develop the EoS having more C_{6+} components than gases from other reservoirs. It is prudent either to refine AGA8-DC92 to accommodate these compositions or to develop a new EoS capable of addressing wider ranges of conditions.[6]

Hydrocarbon dew points for natural gas mixtures are important in contractual specifications throughout the supply chain.[7] Avoiding the formation of liquid in natural gas is critically important. To avoid two-phase flow, it is essential to have reliable data or predictions of the cricondenbar (CB).[8] Phase boundaries of natural gas mixtures are sensitive to small fractions of heavier components, and prediction of the dew point curve with the current EoS appears unreliable.[9]

Custody transfer of natural gas requires an accurate EoS.[10] Simple EoS such as the Soave−Redlich−Kwong (SRK), Peng−Robinson (PR), Patel−Teja (PT), and Benedict−Webb−Rubin (BWR) cannot predict phase boundaries adequately.[11,12] A modified version of the RK,[13,14] Hall−Yarborough,[15] Dranchuk,[16] and Dranchuk et al.[17] are other EoS, but these too lack the ability to predict phase boundaries.

This paper presents data for natural gas-like mixtures that include heavy components. Accurate pressure−density−temperature ($P\rho T$), data are necessary to perform custody transfer of natural gas and to develop a new EoS for industrial and scientific uses. It is also possible to calculate thermal properties from experimental $P\rho T$ data.[18] Knowledge of temperature, pressure, and composition enables determination of the density from an EoS. The American Gas Association developed AGA8-DC92[19] using an extensive and reliable experimental $P\rho T$ database. However the equation is valid only for lean natural gas mixtures over wide ranges of conditions. The equation is only valid for gas phase calculations. This work presents data for a 0.78 mole fraction of a methane mixture that contains heavy components such as might exist in deep water reservoirs.

Experimental Section

This work uses a magnetic suspension densimeter (MSD) for accurate density measurements and an isochoric apparatus for

* Corresponding author. E-mail: mert.atilhan@qu.edu.qa.

10.1021/je100497r
Published on Web 07/07/2010

Table 1. M78C1 Mixture Mole Fractions

component	molar mass g·mol^{-1}	mole fraction
nitrogen	28.01	0.00670
carbon dioxide	44.01	0.00400
methane	16.04	0.77751
ethane	30.07	0.10507
propane	44.10	0.05969
2-methylpropane	58.12	0.01793
butane	58.12	0.00992
2-methylbutane	72.15	0.00495
pentane	72.15	0.00495
hexanes:	86.18	0.00534
n-hexane		0.00218
3-methylpentane		0.00140
2-methylpentane		0.00139
benzene	78.11	0.00030
methylcyclopentane	84.16	0.00007
heptanes:	100.20	0.00284
n-heptane		0.00129
2-methylhexane		0.00050
3-methylhexane		0.00050
toluene	92.14	0.00035
methylcyclohexane	98.19	0.00020
octanes:	114.23	0.0008
n-octane		0.00050
2,2,4-trimethylpentane		0.00030
n-nonane	128.26	0.00030
sum		1.000

phase envelope measurements. The sample mixture has 0.78 mole fraction of methane with numerous other components.

Material. Accurate Gas Products prepared the synthetic mixture used in this work with the composition as presented in Table 1. The gas mixture was prepared gravimetrically with traceability to the National Institute of Standards and Technology (NIST). The estimated uncertainty of the gas mixture is 0.12 %, assuming that the uncertainty comes from the measuring balance and the impurities of the pure gases used in the preparation of the sample.

Isochoric Apparatus for Phase Envelope Measurements. Parts a and b of Figure 1 are schematic diagrams of the isochoric apparatus whose details appear in a previous work.[20] The isochoric apparatus operates between (100 and 500) K with pressures up to 35 MPa. The technique for determining phase loops utilizes the change of the slope of an isochore as it crosses the phase boundary. More details about the isochoric technique can be found in Acosta-Pereza et al.[21] The change of slope does not occur at the cricondentherm (CT), which has a collinear isochore.[22,23] Because the apparatus cell volume changes slightly with pressure and temperature, experimental data require an application of the cell distortion equation to correct the results to isochores. The properties of stainless steel provide a correction for volume distortions with changing temperature and pressure:

$$\frac{V(T,P)}{V(T_0,P_0)} = 1 + \gamma(P - P_0) + \beta(T - T_0) \qquad (1)$$

in which $\gamma = 2.53 \cdot 10^{-5}$ MPa^{-1} and $\beta = 4.86 \cdot 10^{-5}$ K^{-1}.

The system uses isolating vacuum and radiation shields surrounding the cell to reduce energy transmission, to ensure maximum stability and uniformity of temperature within the cell, ± 4 mK, and to minimize the gradients, ± 2 mK. Circulating baths and surrounding heaters enable temperature control. A platinum resistance thermometer with calibration traceable to NIST measures temperature.

A quartz pressure transducer from Paroscientific Inc. measures the pressure, and the manufacturer specifies the uncertainty for the transducer as ± 0.01 % of full scale. The transducer temperature is constant at 343.15 K during measurements, well above the mixture CT. The apparatus uses a fully automated program that allows rapid collection of data. The measurements have evenly spaced isochores, but they emphasize the CT and CB regions. Regularly spaced experimental points on each isochore allow accurate determination of the change in the slope of the isochoric run. The pressure−temperature data along isochores also provides information on mixture density. Knowing the sample mass or at least one density from an external densimeter permits the determination of density along the full isochore. Zhou et al.[20] performed measurements on pure carbon dioxide and propane to verify the capabilities of the isochoric apparatus. Eight vapor pressures of carbon dioxide measured between (230 and 290) K had a maximum relative deviation of ± 0.055 % compared to Span and Wagner[24] and ± 0.04 % when compared to the RefProp 8 as implemented by Lemmon et al.[25] Seven vapor pressures of propane measured between (270 and 340) K had a maximum relative deviation of ± 0.07 % when compared to the same correlation. The estimated uncertainty for the temperature and pressure phase envelope data are 4.5 mK and 0.04 %, respectively.[21]

Single-Sinker Magnetic Suspension Densimeter. Archimedes' principle states "when a solid body is immersed in a fluid, it displaces a volume of fluid the weight of which is equal to the buoyancy force exerted by the fluid on the sinker". This relates the buoyancy force on the submerged object to fluid density. In classical hydrostatic buoyancy densimeters, an object (sinker), usually a sphere or cylinder, hangs from a commercial digital balance by a thin wire. The pressure and temperature of the fluid remains constant in the pressure cell using a temperature control mechanism. The sinker is submerged in the fluid, and the weight of the sinker is measured. According to Archimedes' principle, the density of the fluid is:

$$\rho = \frac{m_v - m_a}{V_s(T,P)} \qquad (2)$$

In eq 2, m_v is the "true" mass of the sinker in vacuum, m_a is the "apparent" mass of the sinker in the fluid, and V_s is the calibrated volume of the sinker, which is a function of temperature and pressure. To overcome limitations in achievable accuracy, the need for frequent calibration of the apparatus with reference fluids, complexity of operation, and restrictions on temperature and pressure, Kleinrahm and Wagner[26] introduced a magnetic suspension device. The novelty of the magnetic suspension coupling was that it used nonphysical-contact force transmission between the sinker in the pressurized cell and the weighing balance at atmospheric pressure, thus allowing a cell design that covered wide temperature and pressure ranges.[27]

Rubotherm Präzisionsmesstechnik manufactured the single-sinker densimeter (Figure 2) used in this work. The Ti sinker used in this work has a volume of 6.74083 ± 0.0034 cm^3 with a 1σ uncertainty of ± 0.05 % and a mass of 30.39157 g, both measured at 293.15 K and 1 bar by the manufacturer. Patil[7] describes operation and details of the instrument. Wagner and Kleinrahm[18] and Kuramoto et al.[28] also provide discussions concerning the operation of these instruments. A Polyscience Inc. model 9512 circulating a heating−cooling bath provides primary temperature control unit. This bath fluid has a temperature operating range of (243 to 393) K. The MSD uses a proportional integral and derivative temperature control implemented by LabVIEW 8.0 as a secondary temperature control unit. Measurements of the high purity pure fluids methane,[29] ethane,[30] and carbon dioxide[31] reveal an uncertainty of less than

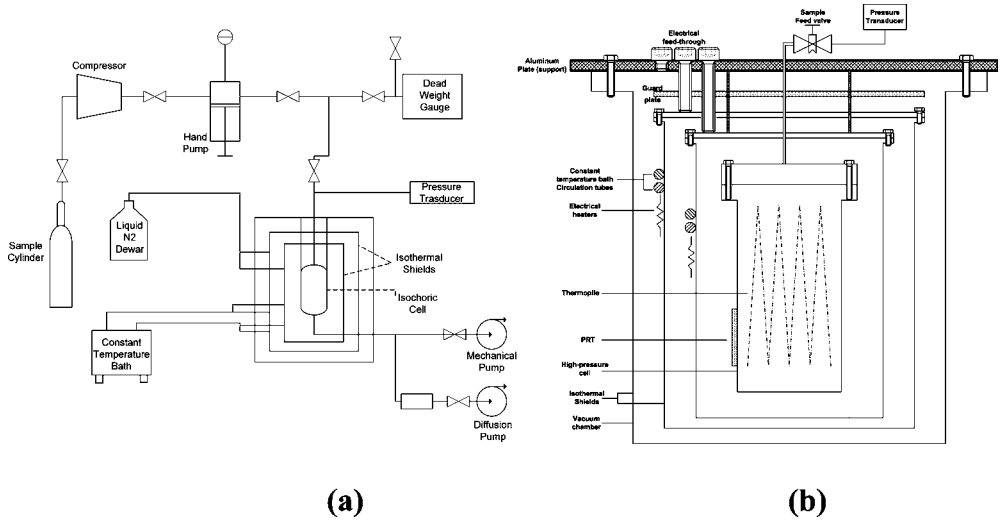

Figure 1. (a) Schematic of isochoric apparatus. (b) Schematic of isochoric cell.

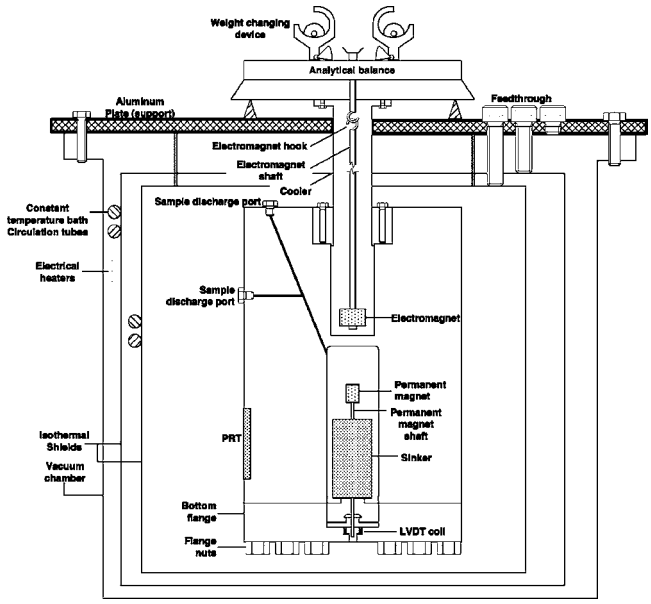

Figure 2. Schematic of the high-pressure magnetic suspension densimeter.

0.05 % over the pressure range up to 200 MPa for density measurements in this apparatus. The force transmission error for the MSD is also studied, and details can be obtained in literature.[32]

Results and Analysis

Isochoric Apparatus Results. This paper contains measurements for 10 isochores over a pressure range of (0 to 35) MPa and a temperature range of (220 to 300) K. The isochoric data for M78C1 are given in Table 2. Table 3 presents the phase boundary data determined for the measured mixture. Figure 3 shows the isochoric apparatus data, experimental phase envelope, and determined values from PR EoS and SRK EoS.

Densimeter Results. Experimental density results and their deviations from AGA8-DC92 and GERG-2004 EoS are in given Table 4. GERG-2004 densities are calculated via REFPROP 8.0 (NIST Reference Fluid Thermodynamic and Transport Properties Database) software available through NIST Thermophysical Properties Division. Density experiments are along four different isotherms at (270, 290, 305, and 340) K. The temperature stability attained across the cell was ± 8 mK at 270 K, ± 10 mK at 290 K, and ± 7 mK at 305 K and at 340 K. The experimental points on each isotherm range up to 34 MPa. The measurements total 27 experimental $P\rho T$ points with the M78C1 with an uncertainty in pressure of 0.01 %. These density measurements are corrected for the force transmission error caused by the magnetic suspension coupling as described by Cristancho et al.[32] Density deviations compared to predictions from AGA8-DC92 appear in Figure 4. The AGA8-DC92 uncertainty ranges are in Table 5. At low temperature and at low pressure the deviations from AGA8-DC92 are more than expected in the original AGA report. It is clear from these results that AGA8-DC92 has problems predicting density at low pressures for the (270, 305, and 340) K isotherms. A closer inspection of data used for AGA8-DC92 development shows

Table 2. M78C1 Isochoric Experimental Pressure and Temperature Data for Isotherms

T/K	*P*/MPa	*T*/K	*P*/MPa	*T*/K	*P*/MPa	*T*/K	*P*/MPa
Isochore 1		Isochore 2		Isochore 3		Isochore 4	
310.15	19.225	330.15	19.347	345.15	18.157	345.15	14.446
305.15	18.327	310.15	16.447	340.15	17.582	340.15	14.033
290.15	15.644	305.15	15.722	330.15	16.430	330.15	13.203
280.15	13.877	290.15	13.548	310.15	14.123	320.15	12.369
275.15	13.002	285.15	12.832	305.15	13.545	310.15	11.531
270.15	12.142	280.15	12.122	300.15	12.968	305.15	11.113
265.15	11.300	275.15	11.420	295.15	12.387	300.15	10.709
262.15	10.810	270.15	10.813	290.15	11.813	296.15	10.408
259.15	10.352	268.15	10.590	285.15	11.259	293.15	10.192
257.15	10.120	265.15	10.282	280.15	10.781	290.15	9.978
				275.15	10.330		
Isochore 5		Isochore 6		Isochore 7		Isochore 8	
345.15	11.116	345.15	8.044	345.15	5.482	345.15	3.843
340.15	10.833	340.15	7.867	340.15	5.377	340.15	3.775
330.15	10.270	335.15	7.690	335.15	5.271	335.15	3.707
320.15	9.701	330.15	7.513	330.15	5.165	330.15	3.639
315.15	9.419	325.15	7.335	325.15	5.059	325.15	3.571
313.15	9.308	320.15	7.159	321.15	4.973	321.15	3.515
310.15	9.150	317.15	7.055	318.15	4.909	318.15	3.474
305.15	8.887	315.15	6.985	315.15	4.844	315.15	3.432
						312.15	3.389

Table 3. Experimental Phase Envelope Points for M78C1

T/K	*P*/MPa
325.1	3.570
322.5	7.242
313.9	9.348
302.1	10.856
286.5	11.425
275.5	11.449
264.5	11.166

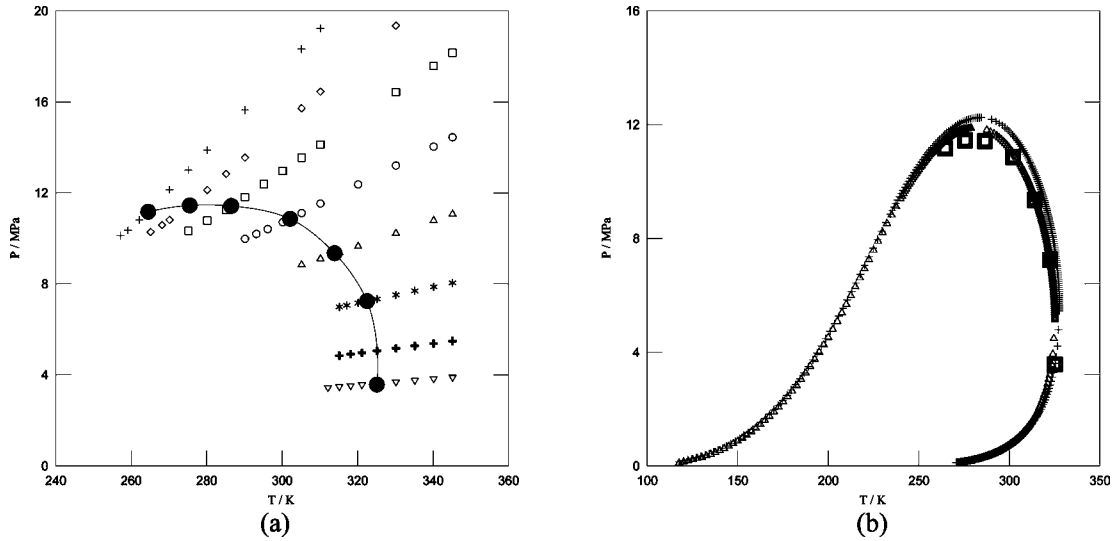

Figure 3. (a) Isochoric experimental data (symbols: +, isochore 1; ◇, isochore 2; □, isochore 3; ○, isochore 4; △, isochore 5; ∗, isochore 6; +, isochore 7; ▽, isochore 8; ●, experimental). (b) Experimental phase envelope and EoS predictions for M78C1 (symbols: +, PR EoS; △, SRK EoS; □, experimental).

Table 4. MSD Density Data for the M78C1 Mixture

temperature		pressure		density			relative deviation	
average	st. dev.	average	st. dev.	exp.	AGA8	GERG-2004	AGA8	GERG-2004
T/K	*T*/mK	*P*/MPa	*P*/MPa	kg·m^{-3}	kg·m^{-3}	kg·m^{-3}	%	%
269.957	14.476	13.783	0.000394	254.227	255.37	257.44	−0.45	−1.25
269.964	6.048	17.234	0.001230	287.442	289.104	288.66	−0.578	−0.42
269.965	6.239	20.7	0.000856	309.565	311.315	309.60	−0.565	−0.01
269.993	9.484	24.132	0.001730	325.686	327.436	325.13	−0.537	0.17
270.004	4.803	27.603	0.001730	338.754	340.348	337.76	−0.471	0.29
269.969	6.921	34.467	0.002690	358.768	360.057	357.35	−0.359	0.40
289.976	13.242	13.788	0.000093	206.922	207.233	208.58	−0.15	−0.79
289.966	7.935	17.241	0.000284	247.293	247.478	248.00	−0.075	−0.29
289.975	7.591	20.69	0.000206	274.851	275.213	274.73	−0.132	0.04
289.957	9.118	24.145	0.000645	295.21	295.692	294.48	−0.163	0.25
289.981	11.462	27.594	0.000435	311.03	311.594	309.93	−0.181	0.35
290.015	8.809	34.471	0.000816	334.881	335.49	333.38	−0.182	0.45
305.045	5.943	13.79	0.000422	178.136	178.953	179.70	−0.459	−0.87
305.02	3.95	17.229	0.000568	218.876	219.486	220.17	−0.279	−0.59
304.983	6.697	20.688	0.001340	249.502	249.832	249.90	−0.132	−0.16
304.992	8.021	24.147	0.001020	272.178	272.656	272.13	−0.176	0.02
305.046	6.398	27.555	0.000763	289.897	290.291	289.32	−0.136	0.20
305.014	9.755	34.5	0.002240	316.911	317.459	315.91	−0.173	0.32
340.031	4.216	3.452	0.000109	28.727	28.783	28.76	−0.194	−0.11
339.979	8.151	6.884	0.000103	61.649	61.849	61.81	−0.325	−0.25
339.956	10.082	10.355	0.000336	98.901	99.042	99.07	−0.143	−0.17
339.988	4.59	13.795	0.000445	136.809	136.686	136.94	0.09	−0.10
339.968	7.489	17.246	0.000364	171.899	171.54	172.00	0.209	−0.06
339.975	7.488	20.69	0.000333	201.797	201.287	201.74	0.253	0.03

that, except for one mixture, the mole fraction of C_{6+} components does not exceed 0.12 %,[33] whereas in this work the total C_{6+} mole fraction is 0.004. Gas mixtures consisting of mostly binary or ternary combinations of methane, ethane, propane, butane, nitrogen, and carbon dioxide are used during the development and validation of AGA8-DC92. Thus, for any natural gas samples or mixtures with C_{6+} higher than the normal or expanded range, the application of AGA8-DC92 is an extrapolation, and the accuracy compared to the normal range mentioned in the original AGA report[19] is questionable.

The total error in density measurements is a combination of random errors and systematic errors. The uncertainty in pressure and temperature measurement, molar compositional analysis, and measurement of the sinker mass under vacuum and at pressure contribute to random error. Systematic error results from uncertainty in sinker volume. This includes uncertainty in sinker volume determination at a reference temperature and pressure, as well as uncertainty in the functional dependence of sinker volume on temperature and pressure. The force transmission error also contributes to systematic error. The error in density caused by pressure, temperature, and composition is:

$$\Delta\rho = \left\{\left[\left(\frac{\partial\rho}{\partial P}\right)_{T,x}\Delta P\right]^2 + \left[\left(\frac{\partial\rho}{\partial T}\right)_{P,x}\Delta T\right]^2 + \sum_{i=1}^{c}\left[\left(\frac{\partial\rho}{\partial x_i}\right)_{P,T,x_{i\neq j}}\Delta x_i\right]^2\right\}^{1/2} \quad (3)$$

The uncertainty caused by the single-sinker densimeter assembly such as sinker volume, balance weightings, and force transmission error are included in the total uncertainty calculations. The total estimated uncertainty of the density measurements is 0.13 %.

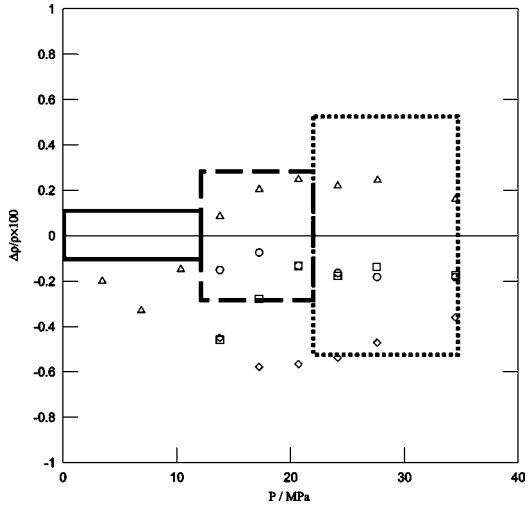

Figure 4. Experimental density deviations from AGA8-DC92 EoS and AGA8 regions. (◇, 270 K; ○, 290 K; □, 305 K; △, 340 K; from left to right: solid line box is AGA uncertainty region 1, long dashed line is AGA uncertainty region 2, fine dashed line is AGA uncertainty region 3).

Table 5. AGA8-DC92 EoS Prediction Ranges

data region	min. *T*/K	max. *T*/K	min. *P*/MPa	max. *P*/MPa
1	265	335	0	12
2	211	394	12	17
3	144	477	17	35

Conclusions

New, accurate experimental data are collected for the phase envelopes and densities of a multicomponent natural gas-like mixture. Phase envelope measurements do not agree with most widely used EoS predictions. Density measurements do not appear to agree with AGA8-DC92 predictions for the industrially important regions. More measurements on multicomponent mixtures containing heavy components appear necessary.

Literature Cited

(1) International Energy Outlook Report, DOE/EIA-0484; Energy Information Administration, U.S. Department of Energy: Washington, DC, 2007.
(2) Worldwide Look at Reserves and Production. *Oil Gas J.* **2005**, *103*, (47), 24−25.
(3) Richardson, G. E.; French, L. S.; Baud, R. D.; Peterson, R. H.; Rorark, C. D.; Montgomery, T. M.; Kazanis, E. G.; Conner, G. M.; Gravois, M. P. Deepwater Gulf of Mexico 2004: America's Expanding Frontier; U.S. Department of the Interior, Mineral Management Service, Gulf of Mexico OCS Region, OCS Report MMS 2004−021: New Orleans, 2004.
(4) Sauer, S. R.; Wiseman, J. Commissioning and Startup of the Caesar and Cleopatra Mardi Grass Deepwater Pipelines, Paper presented at Offshore Technology Conference, Houston, 2006.
(5) International Energy Agency, World Energy Outlook 2009 Edition, 2009. http://www.worldenergyoutlook.org (accessed Jan 2010).
(6) Patil, P. V. Commissioning of a Magnetic Suspension Densitometer for High-accuracy Density Measurements of Natural Gas Mixtures, Dissertation, Texas A&M University, College Station, TX, 2005.
(7) Benton, A. J. Dew Point Measurement. *Hydrocarbon Eng.* **2002**, *7*, 59.
(8) Melvin, A. *Natural Gas: Basic Science and Technology*; Adam Hilger: Philadelphia, PA, 1988.
(9) May, E. F.; Edwards, T. J.; Mann, A. G.; Edwards, C.; Miller, R. C. Development of an Automated Phase Behavior Measurement System for Lean Hydrocarbon Fluid Mixtures, Using Re-entrant Rf/microwave Resonant Cavities. *Fluid Phase Equilib.* **2001**, *185*, 339.
(10) Atilhan, M. A New Cubic Equation of State, Master Thesis, Texas A&M University, College Station, TX, 2004.
(11) Botros, K. K. Performance of Five Equations of State for the Prediction of Vle and Densities of Natural Gas Mixtures in the Dense Phase Region. *Chem. Eng. Commun.* **2002**, *189*, 151–172.
(12) Gharbi, R.; Elsharkawy, A. M. Predicting the Bubble-Point Pressure and Formation-Volume-Factor of Worldwide Crude Oil Systems. *J. Pet. Sci. Technol.* **2003**, *21*, 53–79.
(13) Robinson, R. L.; Jacoby, R. H. Correlation of compressibility factors for gases containing nonhydrocarbons. *Proc. Annu. Conv., Nat. Gas. Process. Assoc., Tech. Pap.* **1965**, *44*, 18–22.
(14) Robinson, R. L.; Jacoby, R. H. Better compressibility factors. *Hydrocarbon Process. Int. Ed.* **1965**, *44*, 141–145.
(15) Yarborough, L.; Hall, K. R. How to solve equation of state for Z-factors. *Oil Gas J.* **1974**, *72*, 86.
(16) Dranchuk, P. M.; Purvis, R. A.; Robinson D. B. Institute of Petroleum Technical Series No. IP 74−008 1, 1974.
(17) Dranchuk, P. M.; Abou-Kassem, J. H. Calculation of Z factors for natural gases using equation of state. *J. Can. Pet. Technol.* **1975**, *14*, 34.
(18) Wagner, W.; Kleinrahm, R. Densimeters for very accurate density measurements of fluids over large ranges of temperature, pressure, and density. *Metrologia* **2004**, *41*, S24–S39.
(19) Compressibility Factors of Natural Gas and Other Related Hydrocarbon Gases, American Gas Association, Annual Report No. 8, Washington, DC, 1992.
(20) Zhou, J. J.; Patil, P. V.; Ejaz, S.; Atilhan, M.; Holste, J. C.; Hall, K. R. (p, V_m, T) and phase equilibrium measurements for a natural gas-like mixture using an automated isochoric apparatus. *J. Chem. Thermodyn.* **2006**, *38*, 1489–1494.
(21) Acosta-Pereza, P.; Cristancho, D. E.; Mantilla, I. D.; Hall, K. R.; Iglesias-Silva, G. A. Method and uncertainties to determine phase boundaries from isochoric data. *Fluid Phase Equilib.* **2009**, *283*, 17–21.
(22) Eubank, P. T.; Barrufet, M. A. General conditions of collinearity at the phase boundaries of fluid mixtures. *AIChE J.* **1987**, *33*, 1882–1887.
(23) Eubank, P. T.; Joffrion, L. L.; Patel, M. R.; Warowny, W. Experimental densities and virial coefficients for steam from 348 to 498 K with correction for adsorption effects. *J. Chem. Thermodyn.* **1988**, *20*, 1009–1034.
(24) Span, R.; Wagner, W. A New Equation of State for Carbon Dioxide Covering the Fluid Region from the Triple-Point Temperature to 1100 K at Pressures up to 800 MPa. *J. Phys. Chem. Ref. Data* **1996**, *25*, 1509–1596.
(25) Lemmon, E. W.; Huber, M. L.; McLinden, M. O. *NIST Reference Fluid Thermodynamic and Transport Properties REFPROP, Version 8.0*; National Institute of Standards and Technology, Standard Reference Data Program: Gaithersburg, MD, 2007.
(26) Kleinrahm, R.; Wagner, W. Development and Design of a Density Measuring Arrangement for Measuring the Boiling and Thawing Densities of Pure Fluid Materials over the Whole Phase Boundary Curve. *Prog. Rep. VDI J.* **1984**, *3*, 92.
(27) Lösch, H. W. *Development and Design of New Magnetic Suspension Balances for Non-Contact Measurements of Vertical Forces*; VDI Verlog: Dusseldolf, 1987.
(28) Kuramoto, N.; Fujii, K.; Waseda, A. Accurate density measurements of reference liquids by a magnetic suspension balance. *Metrologia* **2004**, *41*, S84–S94.
(29) Cristancho, D. E.; Mantilla, I. D.; Ejaz, S.; Hall, K. R.; Atilhan, M.; Iglesia-Silva, G. A. Accurate $P\rho T$ Data for Methane from (300 to 450) K up to 180 MPa. *J. Chem. Eng. Data* **2010**, *55*, 826–829.
(30) Cristancho, D. E.; Mantilla, I. D.; Ejaz, S.; Hall, K. R.; Atilhan, M.; Iglesias-Silva, G. A. Accurate $P\rho T$ Data for Ethane from (298 to 450) K up to 200 MPa. *J. Chem. Eng. Data* **2010**; DOI: 10.1021/je900978x.
(31) Mantilla, I. D.; Cristancho, D. E.; Ejaz, S.; Hall, K. R.; Atilhan, M.; Iglesia-Silva, G. A. P-ρ-T Data for Carbon Dioxide from (310 to 450) K up to 160 MPa. *J. Chem. Eng. Data* **2010**; DOI: 10.1021/je1001158.
(32) Cristancho, D. E.; Mantilla, I. D.; Ejaz, S.; Hall, K. R.; Iglesias-Silva, G. A.; Atilhan, M. Force Transmission Error Analysis for a High-Pressure Single-Sinker Magnetic Suspension Densimeter. *Int. J. Thermophys.* **2010**; DOI: 10.1007/s10765-010-0702-3.
(33) Savidge, J. L.; Beyerlein, S. W.; Lemmon, E. W. Technical Reference Document for the 2nd Edition of AGA Report No. 8, Gas Research Institute: Des Plaines, IL, Topical Report No. GRI-93/0181, 1995.

Received for review May 11, 2010. Accepted June 17, 2010. The authors express their gratitude to Mardi Gras Transportation Systems, LLC for the funding provided. The authors also also appreciate support from Premier Measurement Services and Savant Measurement Corporation. Financial support also came from the Texas Engineering Experiment Station and the Jack E. & Francis Brown Chair funds.

JE100497R